CHARACTERIZATION OF A SMALL, MATURE OIL RESERVOIR WITH LIMITED DATA: A CASE STUDY OF THE ROUND TANK QUEEN FIELD

Srichumsin, Akapak; Engler, Thomas W.
New Mexico Tech

ABSTRACT

A common problem in small, mature fields is the limited and poor quality data, typically consisting of only old logs and production history. The objective of this work is to demonstrate practical applications for processing and analyzing the limited information. The Round Tank (Queen) reservoir in Southeast, New Mexico was selected as a case study. Old logs, 14 modern logs and one-core are the main sources for this reservoir study. The results from modern-log analysis will be used to support the results obtained from the old logs. Normalization of old neutron logs and calibration of old sonic logs were two techniques applied to acquire valuable information. As a result the mineralogy, porosity and productive thickness of the Queen were determined. A newly discovered friable sand bed was identified and has implications on stimulation and reservoir performance. The reservoir characterization can be further used for field optimization or EOR project.

INTRODUCTION

A common problem in small, mature fields is the limited and poor quality data, typically consisting of only old logs and production history. The objective of this study is to demonstrate practical applications for processing and analyzing the limited information. The Round Tank (Queen) reservoir in Southeast, New Mexico was selected as a case study.

The Round Tank Queen reservoir is one of the porous, productive hydrocarbon lenses in the Queen formation. The structure is a terrace shape with updip/downdip in the west/east direction **(Figure 1).** Oil and gas are trapped by the loss of porosity in updip and downdip directions coupled with the anhydrite layers on top and bottom of the productive zone. A large gas cap exists on top of thin oil column. The reservoir is small (~16 ft thick), shallow (~1,500 ft depth), low temperature (75°F), and has an unfavorable mobility ratio. Through time, reservoir pressure has depleted from 600 psia to ~50 psia. The field started to produce from the Queen formation in January 1970. A total 9 wells have produced from the Round Tank Queen reservoir; 6 wells produced from the gas cap, and 3 wells produced from the oil column. Original oil-in-place is approximately 2.85 million barrels. Cumulative oil and gas production are 26,502 BO and 4.2 Bscf, respectively.

Evaluation of this field relies on existing data or data which are easy to acquire; high cost information such as seismic and special wireline logging are not available. Old logs (circa 1960s), 14 modern logs and one-core are the main sources for this reservoir study. The main problems applying old logs are (1) the poor quality and reliability and (2) the required conversion of the neutron logs from API or CPS scale to porosity units. The following sections provide applications for improving unreliable and poor quality data to useful and reliable data. Mineralogy of the Round Tank Queen formation was also observed through modern logs coupled with a thin section study from the core samples.

DATA ACQUISITION

This paper focuses on data acquisition from wireline logs which includes porosity and lithology. Other parameters acquired from the core experiments such as permeability, relative permeability curves, and capillary pressure curve are not included in this paper, but are detailed in Srichumsin (2011).

Porosity

Porosity logs are separated into two groups – modern logs (late 2000s) and old logs (1960s to 1970s). Basically, the results from modern-log analysis will be used to calibrate and support the results obtained from the old logs. Normalization of old neutron logs and calibration of old sonic logs were two techniques applied to acquire valuable information.

I.) Modern logs

The modern logs are available from fourteen wells that have recently been drilled to the deeper San Andres target. Ten wells, Eskimo State No.1 to No.10, have a complete logging set which are gamma ray, caliper, resistivity, litho-density, density, and neutron logs. The remainder has only gamma ray and neutron.

Density/neutron crossplot is applied to calculate true porosity. **Figure 2** compares the true porosity curves using the top of the Queen formation as datum. Two observations can be made from the comparison. First, the curve trends are similar; (1) the low porosity intervals on top and bottom of the formation are due to anhydrite layers, (2) if dividing the sand into two sections equally (top and bottom), porosity of the bottom section is higher than the top section. Second, the locations and values of minimum and maximum porosities are fairly consistent; (1) minimum porosities are in the anhydrite layers, and (2) maximum porosities are located approximately 10 to 13 ft below the formation top.

II.) Old logs

Three types of porosity log are available – neutron, density, and sonic logs. Only one type is available for most old wells. The following sections focus on the acquisition of porosity from neutron and sonic logs.

Neutron logs: A common problem for the old neutron log is the units; generally, CPS or API unit was used. These units, typically, can be converted to porosity unit (either % or fraction) with the use of calibration chart provided by a logging company. In the Round Tank Field, neutron logging was operated by different companies with different scale-ranges, borehole conditions, and calibrations. Thus, using a calibration chart to obtain true porosity is not practical. In general, if the proper calibration chart is not accessible, conversion can be made from an empirical correlation of tool response and core porosity. Then, the correlation can be applied to other wells in a field that have similar conditions. In the case when lacking core data, a linear relationship of tool response and porosity can be created from two known, porosity control points (Bassiouni 1994).

The second method, a porosity-unit transform by linear relationship of tool response and porosity, is applied in this study because of the lack of core data to generate a relationship and too many neutron-logging companies operating in the field. One main concern about this method is that only one control point is assured, which is porosity/tool-response at the anhydrite layer. Therefore, another control point needs to be clarified. To do so, comparison among neutron logs has to be made to investigate any common point that can be identified. All the logs with various scale-ranges were normalized into *0-1* scale-range with a linear relationship (Eq.1); the minimum tool response (maximum porosity) in the Queen formation is set to *1*, and the maximum tool response (minimum porosity) is set to *0*. **Figure 3** demonstrates the results after normalization.

$$N_x = \frac{(T_x - T_{\max})}{(T_{\min} - T_{\max})} \quad , \ldots\ldots (1)$$

The figure shows that the positions of the maximum value or *1* from each normalized curve are approximately 12 to 15 ft below the top of the Queen formation. These locations are aligned with the positions of the maximum porosity calculated by modern logs. As a result, average maximum porosity from modern logs is chosen to be the second control point for creating the linear relationship; the average maximum porosity is 23.4%.

Two linear relationships were made: (1) linear porosity vs. linear tool response, Eq.2 (2) log porosity vs. linear tool response, Eq.3. **Figure 4** illustrates the comparison between these two relationships in the semi-log scale.

$$\phi_x = \frac{(T_x - T_{\min})(\bar{\phi}_{\max} - \bar{\phi}_{\min})}{(T_{\max} - T_{\min})} + \bar{\phi}_{\min} \quad , \ldots\ldots (2)$$

$$\log\phi_x = \frac{(T_x - T_{\min})(\log\bar{\phi}_{\max} - \log\bar{\phi}_{\min})}{(T_{\max} - T_{\min})} + \log\bar{\phi}_{\min} \quad , \ldots\ldots (3)$$

$\bar{\phi}_{\max}$ and $\bar{\phi}_{\min}$ for this study are 0.234 and 0.01 respectively.

The second relationship, log porosity vs. linear tool response, provided better matching results when compared with adjacent wells (see example in **Figure 5**). It can be observed that the linear/linear relationship over-predicts the porosity values that are between two controlling points. **Figure 6** shows the final results for nine wells with neutron logs.

A linear relationship between log porosity and linear neutron-logging tool response was found in many cases, including in Permian Basin observations in the early 1950s (Frank 1986). Furthermore, another advantage from this method is that the normalizing process helps to mitigate the effects of the different conditions among wells such as hole size, mud type, and logging company. Therefore, the results obtained from this method are more concrete, and hence improve unreliable and poor quality data to useful and reliable data.

Sonic logs: Two types of sonic logs for the field are Basic Sonic and Borehole Compensated Sonic (BHC); thus, only compressional wave data are available for characterizing the reservoir. Based on tool response, the interval transit time (*t*), in the Queen interval, sonic logs can be separated into 3 groups–High *t*, Moderate *t*, and Low *t* (see details in **Table 1**). The interval transit time is normally recorded in a range of 44 μsec/ft to 190 μsec/ft, from dense dolomite with 0% porosity to fresh water with 100% porosity. However, the maximum tool responses from High *t* and Moderate *t* groups show very high interval transit time, 97 μsec/ft to 143 μsec/ft, in both gas and oil zones (see Table 1 for details). In general, abnormally high interval transit time is due to the effect of reservoir gas and uncompacted formation. Alberty (1994) shows in his paper that apart from compaction of the formation, many factors can affect the arrival time of compressional wave such as water salinity, dissolved gas saturation, temperature, pressure, water saturation, and hydrocarbon properties. However, after studying through Alberty's experimental results and comparing with the Round Tank Queen reservoir conditions, those factors insignificantly affect the tool response. Core samples collected from Round Tank Queen Unit No.6-Y **(Figure 7)** has indicated friable characteristic of the formation. Note that this well is located in proximity to the High *t* well (State Mullis B No.1) as well. Thus, it can be concluded that the high tool responses are mainly from the effect of friable rock.

In 1956, Wyllie et al. proposed the method for calculating porosity from interval transit time by time-average relationship.

$$\phi_w = \frac{t_{\log} - t_{ma}}{t_f - t_{ma}} \ , \qquad \text{(4)}$$

The method is based on the assumption that only rock matrix and fluid properties affect wave velocity which consequently leads to the limitation of the method to be precise only for clean, consolidated, and uniformly distributed small pore formation. In 1980, Raymer et al. proposed the empirical transform which was based on field observations:

$$\phi_R = C\left(\frac{t_{\log} - t_{ma}}{t_{\log}}\right) , \qquad \text{(5)}$$

Where C = 0.6 for gas zone, C = 0.67 for oil and water zones, and t_{ma} = 56 μsec/ft for sandstone formation.
The equation is accepted to be more suitable for unconsolidated/friable formations rather than Wyllie transform; therefore, the Raymer-Hunt transform is applied in this study due to the observed high *t* trend and friable characteristic of the rock.

However, even though Raymer-Hunt transform has been applied, the calculated porosities are still much higher than expected when comparing with adjacent wells **(Figure 8).** Bassiouni (1994) also shows that unconsolidated sands from Gulf of Mexico do not comply with the Raymer-Hunt transform; where the actual porosities from core experiment tend to be lower than calculated. It is possible that Raymer-Hunt transform is not applicable within the Round Tank Queen formation. Thus, an additional calibration is required to estimate reliable porosity values from sonic logs.

Overestimated porosities due to the effect of friable sand need to be re-calibrated. The work was done by applying an Uncompaction Correction (U_c) to the Raymer-Hunt transform. U_c is the ratio of apparent sonic porosity to known porosity; the known porosity can be obtained from the maximum porosity in the Queen interval from adjacent new wells. The maximum porosity values were selected because they provided the most consistent values through the Queen interval (stated previously in *Modern logs* and *Neutron logs* sections). Therefore, the number used for the apparent sonic porosity has to be the maximum porosity in the Queen formation calculated by Raymer-Hunt transform. The equation becomes

$$U_c = \frac{\phi_{R(\max)}}{\phi_{known(\max)}} \ , \qquad \text{(6)}$$

Then, true porosity can be calculated from

$$\phi_R' = \frac{\phi_R}{U_c} \ , \qquad \text{(7)}$$

Nevertheless, not all the wells with sonic logs are in proximity to the wells with modern-log analysis. Only one or two wells from each group - High *t*, Moderate *t*, and Low *t* - are adjacent to the wells with modern logs. Therefore, U_c is calculated from a representative well and is applied to the rest in the group. The U_c numbers are 1.64, 1.25, and 1.05 for High *t*, Moderate *t*, and Low *t*, respectively. **Figure 9** illustrates the comparison between the modified Raymer-Hunt transforms with published Gulf of Mexico data obtained from moderately consolidated to unconsolidated sands (Hartley 1981). It can be observed that the relationship of High *t* group seems to be too low. To avoid over reduction of porosity, U_c is limited at 1.33 (the number obtained from the maximum possible U_c that matches published data). Table 1 summarizes all the information for calculating porosity from sonic logs. **Figure 10** compares the results after calibrating friable-sand effect with porosities from the adjacent wells. Also, **Figure 11** summarizes the final results from all sonic logs. As seen in the figures, the proposed procedure gives satisfactory results in both value and curve trend. Moreover, the wells that use U_c from a representative well also exhibit reasonable outcomes.

Lithology

Layer: To describe fluid flow in the Queen Sand reservoir requires accurate definition of the geologic flow units within the sand. A stratigraphic layering approach was chosen to identify the number of layers and layer thicknesses. The work was done by applying gamma ray logs as the main source for classifying layers. The reason of using gamma ray logs is they provide a more appropriate description for reservoir stratigraphy and geology than using porosity logs. Gamma ray logs are not affected by porosity pinchout, and the curve trends are quite consistent across the field. In **Figure 12**, gamma ray logs are plotted along with porosity logs of Eskimo State No.1 to No.9 to show the consistent layering in the sand.

As a result, the Round Tank Queen sand can be divided into three layers based on gamma ray values, with Layer3 containing the highest gamma ray responses followed by Layer1 and Layer2, respectively. After layers have been identified, two geologic properties, porosity and thickness, can be observed. The results are as follows: (1) Layer3 has the highest porosity values among all layers, and (2) the thickest layer is Layer3 followed by Layer1 and Layer2, respectively.

Mineralogy: Mineralogy of the Round Tank Queen sand has been studied through examination of core samples and interpretation of wireline logs. Figure 7 shows a core sample along with gamma ray and neutron logs from Round Tank Queen Unit No.6-Y. A thin section study was done by Wilson (2010) on a sample taken from the core at 1,492 ft depth. The results show that the main mineral is quartz, mixed with potassium feldspar and anhydrite. Scanning Electron Microscope (SEM) images were taken from two core samples at depths of 1,493.2 ft and 1,502 ft. The SEM results from 1,493.2 ft section reveal that the rock also contains some dolomite, calcite, micas, and illite. For the sample at 1,502 ft, anhydrite is the main mineral; as expected since the section is located at the very bottom part of the Round Tank Queen sand.

Mineralogy analysis through wireline logs was made by using density/neutron crossplot and lithodensity MID plot. Density, neutron, and Pe logs from Eskimo State No.1 to No.9 were used to generate the plots. The results are similar for all the analyzed wells. **Figure 13** shows an example of the plots from Eskimo State No.2. Two observations can be made from the plots: (1) anhydrite layers exist on the top and bottom of the productive interval, and (2) quartz is the main mineral of the formation; similar to the core study, with other minor minerals present a combination of potassium feldspar, anhydrite, micas, and illite.

Mineral identification was also made through gamma ray spectrometry tool with the assistance of Schlumberger mineral identification chart **(Figure 14).** The chart, basically, is used to determine the type of radioactive minerals in a shaly formation from potassium and thorium concentrations measured by the gamma ray spectrometry tool. Details of thorium and potassium concentrations are available in three wells – Eskimo State No.1, No.2, and No.7. The main objectives for this task are (1) to identify the type of radioactive minerals in the formation and (2) to determine mineral differences between layers. To achieve the second goal, representative positions for each layer need to be clarified. The criteria are as follows: (1) for Layer1 and Layer3, the position is selected at the maximum gamma ray response, and (2) for Layer2, the minimum gamma ray response position is chosen. Figure 14 illustrates the results after overlaying data points into the chart. Three observations can be made from the figure. First, most of the data points fall within micas region. This result does not mean that the main radioactive mineral is micas, but this trend could have been due to the effect of the formation consisting of many clay minerals. However, the points still fall within the expected range, between feldspar and illite regions (0.3 Th/K to 3.5 Th/K), which supports the previous SEM analysis about rock composition. The second observation is that Layer3 contains the largest amount of clay minerals in the formation followed by Layer1 and Layer2, respectively. Third, thorium/potassium ratios (Th/K) are quite consistent among layers (~1.7 Th/K). This indicates that constituents of clay minerals are quite similar among layers.

DATA INTERPRETATION

Identification of friable zone

Evidence indicates that a friable zone exists with the Queen sand. The sonic log responses were used for this study to observe the trend. As stated previously, sonic logs in some wells show abnormally high responses (high interval transit time) which could indicate that the formation around those areas are not compact.

The observation was made by focusing on two dimensions – areal and vertical. For the areal dimension, the characteristics of the tool response, High *t*, Moderate *t*, and Low *t*, from all the wells were mapped out to observe the trend. **Figure 15** demonstrates the mapping result from all thirteen wells that have sonic logs. The figure indicates that all of the High *t* and Moderate *t* wells are located in the northern part of the field; while on the other hand, most of the Low *t* wells are located in the southern part of the field. Therefore, it is postulated that the formation in the northern part of the field is more friable than the southern part. For the vertical dimension, gamma ray and sonic logs from High *t* wells were used to identify friable characteristics of the rock between layers. The gamma ray log was used to identify layers, and sonic log to determine the level of rock compaction. **Figure 16** shows the analyzed results from three High *t* wells – State Mullis B No.1, Mehurin No.1, and Mehurin No.3. It can be observed that interval transit time from Layer3 seems to have the highest over-response followed by Layer2 and Layer1, respectively.

A core sample from Round Tank Queen Unit No.6-Y (Figure 7) also supports the above analysis that Layer3 is the most friable interval. Note that this well is located in the friable area and in proximity to State Mullis B No.1 (280 ft apart) where the sonic log shows high interval transit time. It can be observed from the collected core that the main productive interval (Layer3 in the figure) is missing. This section could have been washed out during coring operation because of the friable characteristic. The core sample that could be collected and analyzed is located in Layer2, above the missing zone. Even though the sample from this section is tighter and has less friable characteristics than the missing interval, the rock still reveals softness and friable characteristics. Unfortunately, due to the unexpected uplift of the Round Tank Queen formation at this well location, the coring operation missed collecting a core sample at the top section of the formation (Layer1).

Improvement of reservoir description

The previous works in *Data acquisition* section have significantly improved reservoir description in many ways, especially porosity distribution. This section provides an example through porosity maps. Three porosity maps of the Round Tank Queen sand (Layer3) were generated with different sources: (1) Map1: porosity map from old logs (2) Map2: porosity map from old logs and modern logs (3) Map3: porosity map from calibrated old logs and modern logs. All maps were generated by a commercial software. The Kriging method was selected as the geostatistical technique for interpolating and extrapolating unknown values in the area of no observation. Layer3 was selected to represent porosity distribution of the formation because of its consistency in porosity and thickness. Note that porosity information from most of neutron logs were not included in Map1 and Map2; the reason is to resemble an actual condition if no calibration is made. **Figure 17** shows the comparison between Map1, Map2, and Map3; thus, illustrating the improvement made by modern logs and the proposed applications. Pore volumes of the productive area (summation of sections 19, 24, 25, and 30) calculated from Map1, Map2, and Map3 are 182×10^6 ft^3, 174×10^6 ft^3, and 160×10^6 ft^3; i.e., a 12 % reduction in pore volume.

Two observations can be made from the figure. First, modern logs and calibrations of the old sonic logs help to mitigate the overestimation of porosity due to the effect of friable characteristics. It can be seen from Map1 that high porosity region (> 25% porosity) covers most of the productive area. Once modern logs and calibrated sonic logs were applied, the result, Map3, shows a satisfactory outcome. Furthermore the map also preserves the details of the friable zone; i.e., the northern part contains higher porosity than the southern part. Second, modern logs and normalization of the old neutron logs help to obtain details for reservoir description. For instance, Map3 reveals the heterogeneity of porosity at JW-State No.2 (2300FSL 682FWL 30 T15S R29E) where this trend does not exist in Map1 and Map2 due to the lack of information from old neutron logs.

TECHNICAL CONTRIBUTION

The applications proposed in this paper are simple, easy to apply, and do not require high cost information. An improvement of the Round Tank Queen reservoir description was accomplished with the limited data: old logs, 14 modern logs, and one core. The applications presented in this paper would be of help to characterize a field with similar problems: (1) old sonic logs show abnormally high tool responses and/or (2) unable to convert CPS or API units of old neutron logs to porosity units. However, to be able to apply the applications, two control points of a formation need to be identified. Lastly, the improved reservoir description can be further used for field optimization or EOR project. A simulation model can be constructed with better reservoir characterization, and consequently more precise prediction results can be obtained.

CONCLUSIONS

Successful characterization of the Round Tank Queen reservoir with limited and poor quality data was made with the assistance of modern logs and core analysis. Normalization of old neutron logs and calibration of old sonic logs were two techniques applied to acquire valuable information. As a result the mineralogy, porosity and productive thickness of the formation were determined. The study of mineralogy from wireline logs and core samples indicates that quartz is the main mineral of the formation with other minor minerals present a combination of potassium feldspar, anhydrite, micas, and illite. A newly discovered friable sand bed was also identified and has implications on stimulation and reservoir performance.

NOMENCLATURE

C = constant parameter for Raymer-Hunt transform, dimensionless
N_x = normalized neutron-logging tool response at interested depth, dimensionless
t = interval transit time, μsec/ft
t_f = fluid interval transit time, μsec/ft
t_{log} = apparent interval transit time, μsec/ft
t_{ma} = matrix interval transit time, μsec/ft
T_x = neutron-logging tool response at interested depth, CPS [API]
T_{max} = maximum neutron-logging tool response at interested interval, CPS [API]
T_{min} = minimum neutron-logging tool response at interested interval, CPS [API]
U_c = Uncompaction correction, dimensionless
$\phi_{known(\max)}$ = maximum porosity from modern-log analysis, frac.
ϕ_R = porosity from Raymer-Hunt transform, frac.
$\phi_{R(\max)}$ = maximum porosity from Raymer-Hunt transform, frac.
ϕ_R' = true porosity from modified Raymer-Hunt transform, frac.
ϕ_w = porosity from Wyllie equation, frac.
ϕ_x = porosity at interested depth, frac.
$\bar{\phi}_{\max}$ = average maximum porosity, frac.
$\bar{\phi}_{\min}$ = average minimum porosity, frac.

REFERENCES

Alberty, M. 1994. *The Influence of the Borehole Environment Upon Compressional Sonic Logs*, presented at the 1994 SPWLA Annual Logging Symposium.

Bassiouni, Z. 1994. *Theory, Measurement, and Interpretation of Well Logs*, Textbook Series Vol.4, SPE, Richardson, Texas.

Frank, R.W. 1986, *Prospecting With Old E-Logs*, Schlumberger, Houston, Texas.

Hartley, K.B. 1981. Factors Affecting Sandstone Acoustic Compressional Velocities and an Examination of Empirical Correlations Between Velocities and Porosities, paper PP presented at the 1981 SPWLA Annual Logging Symposium, June.

Log Interpretation Chart, Schlumberger, Houston, Texas.

Raymer, L.L., and Hunt, E.R. 1980. *An Improved Sonic Transit Time-to-Porosity Transform*, paper P presented at the 1980 SPWLA Annual Logging Symposium, July.

Srichumsin, A. 2011. *Study Mini-Waterflood Potential of The Round Tank Queen Reservoir, Chaves County, New Mexico through Reservoir Simulation*, MS thesis, New Mexico Inst. of Mining and Tech., Socorro, New Mexico.

Wilson, G.A. 2010. *Core Analysis of the Round Tank Queen Reservoir, Chaves County, New Mexico*, MS thesis, New Mexico Inst. of Mining and Tech., Socorro, New Mexico.

Wyllie, M.R.J., Gregory, A.R., and Gardner, G.H.F. 1956. "Elastic Wave Velocity in Heterogeneous and Porous Media", *Geophysics* (Jan. 1956) **21**, No.1, 41-70.

ACKNOWLEDGMENTS

We would like to acknowledge Research Partnership to Secure Energy for America (RPSEA) for providing the funding for this project. We greatly appreciate Armstrong Energy for contributing their time and effort to obtain significant resources, especially the acquisition of core. We also would like to thank the Petroleum Recovery Research Center (PRRC) for their great support with the core experiments. The work was accomplished with the use of various software packages: NeuraLog, Surfer® and *LESA*. We are thankful to Neuralog, Golden Software and Digital Formation for providing the academic licenses to the Department of Petroleum and Natural Gas Engineering, New Mexico Tech.

TABLE 1 - PARAMETERS AND VALUES FOR CALCULATING TRUE POROSITY FROM SONIC LOGS

Well	No.	t_{max} (μsec/ft)	Zone	C	t_{ma} (μsec/ft)	U_c
High t						
STATE-MULLIS B *	1	131	Oil	0.67	56	1.33
MEHURIN	1	128	Gas	0.6	56	1.33
MEHURIN	3	143	Gas	0.6	56	1.33
MULLIS-STATE A	1	123	Gas	0.6	56	1.33
Moderate t						
FEDERAL *	2	99	Oil	0.67	56	1.25
USA-FITZGERALD *	2	98	Oil	0.67	56	1.25
USA-FITZGERALD	4	97	Oil	0.67	56	1.25
USA-MEHURIN	2	100	Gas/oil	0.6/0.67	56	1.25
USA-MEHURIN	4	104	Gas	0.6	56	1.25
Low t						
STATE A *	1	89	Oil/water	0.67	56	1.05
STATE A *	2	86	Water	0.67	56	1.05
FEDERAL	1	83	Water	0.67	56	1.05
USA-FITZGERALD	3	92	Oil/water	0.67	56	1.05

* Calibration well

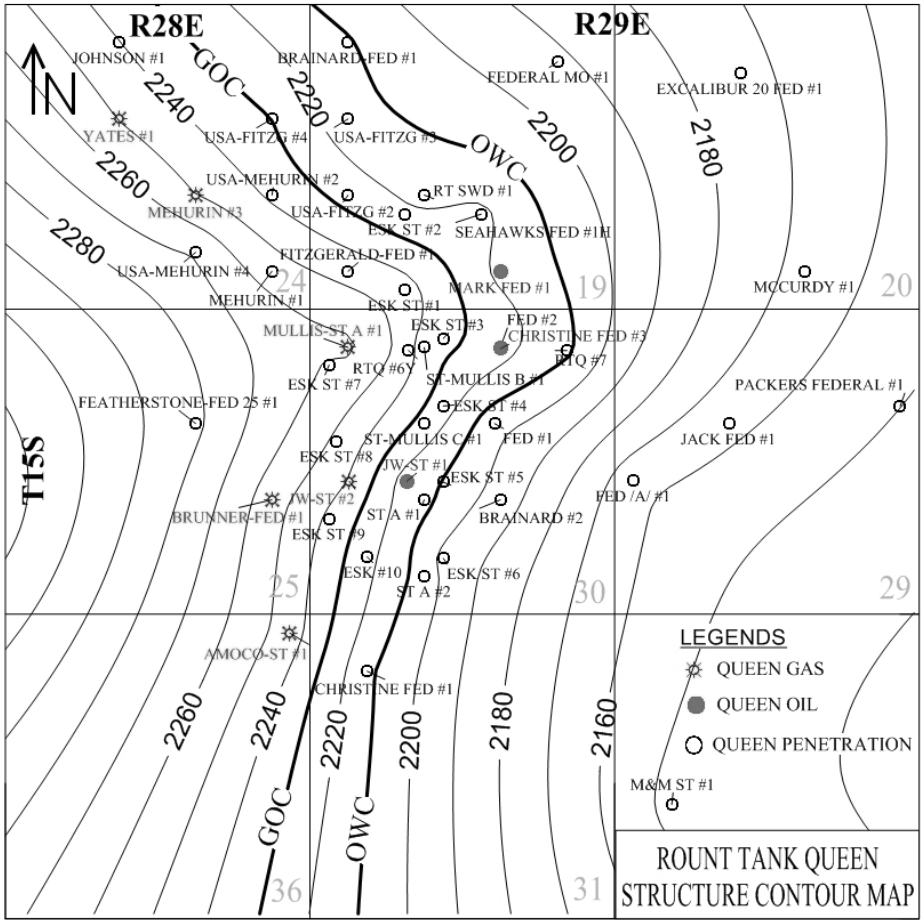

Figure 1 - Structure contour map of the Round Tank Queen formation

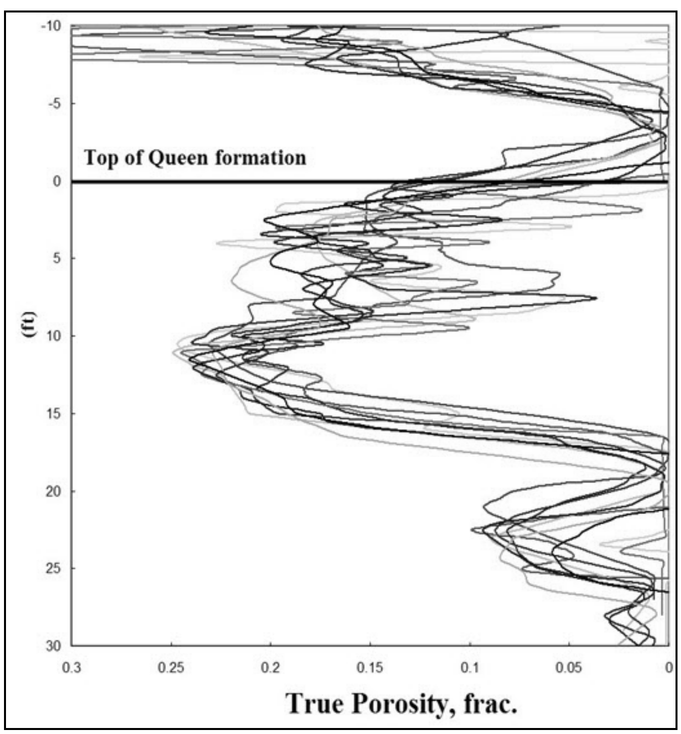

Figure 2 - True porosity from modern logs

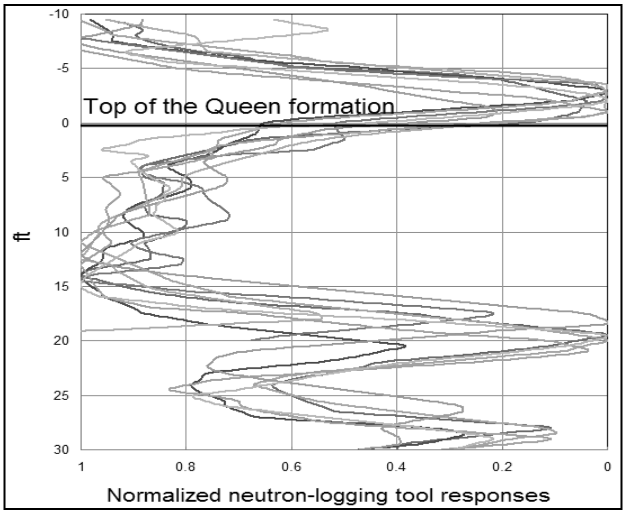

Figure 3 - Normalized neutron logs

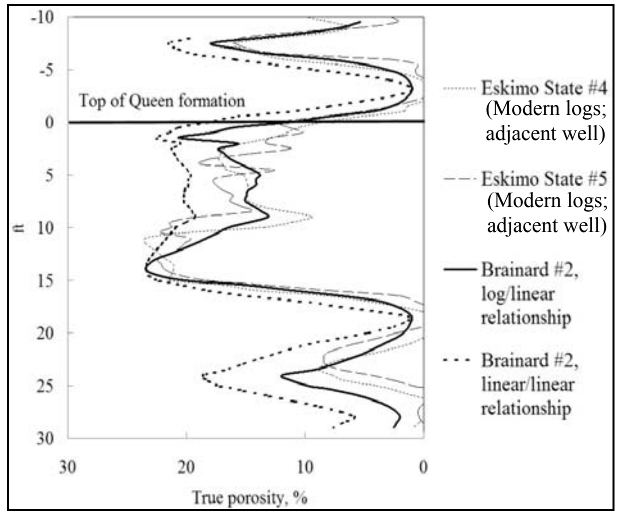

Figure 5 – Comparison of porosity obtained from linear relationships and from modern logs

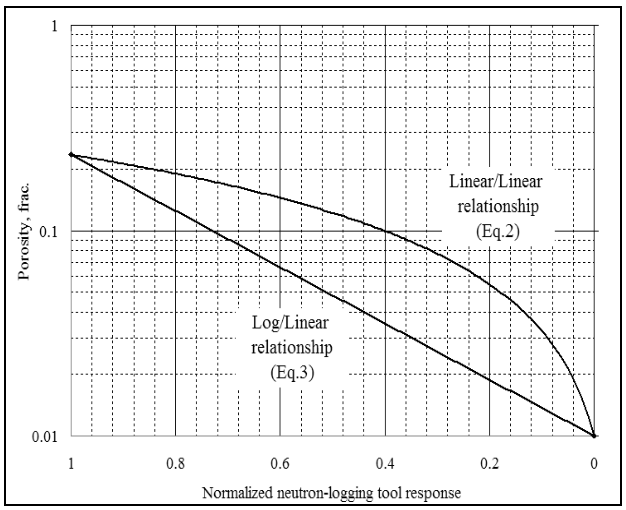

Figure 4 – The comparison between linear/linear and log/linear relationships

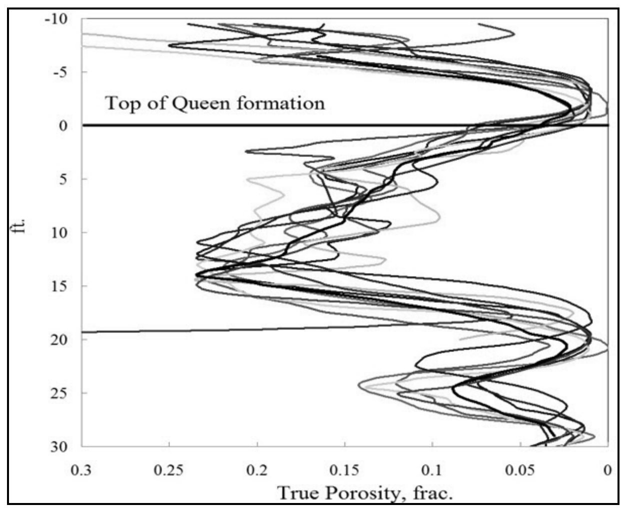

Figure 6 – True porosity from old neutron logs

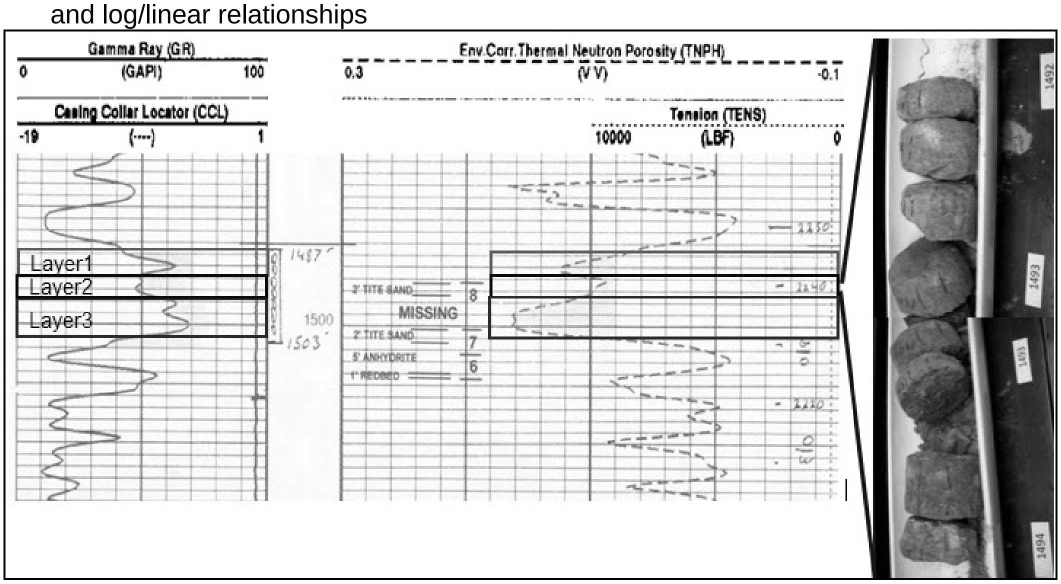

Figure 7 – Gamma ray log, neutron log, and core sample of Round Tank Queen Unit No.6-Y

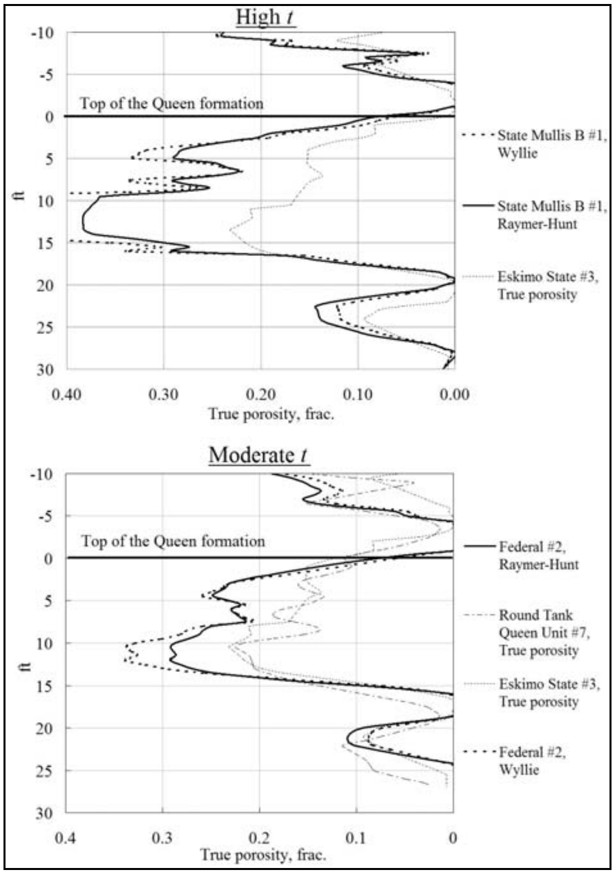

Figure 8 – Overestimated porosity from Wyllie and Raymer-Hunt transforms

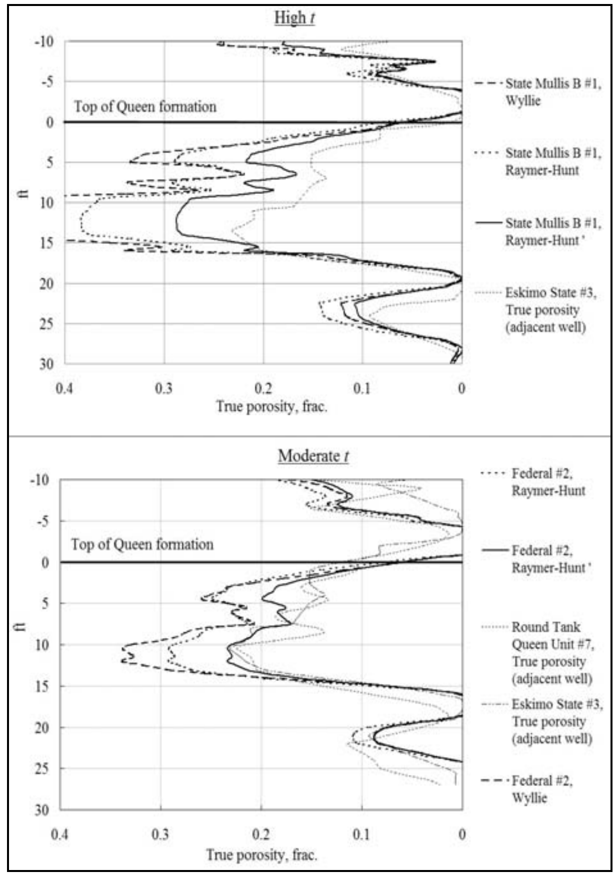

Figure 10 - Comparison of porosity between modified Raymer-Hunt transform and adjacent wells

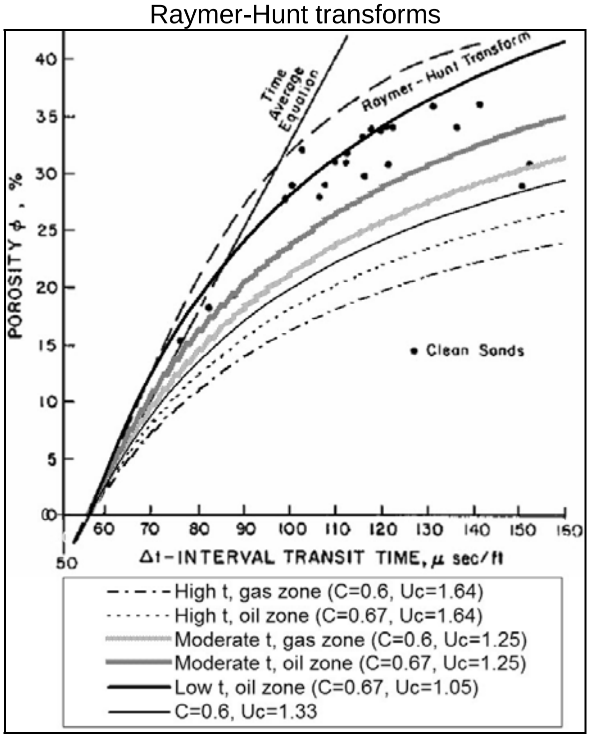

Figure 9 – Comparison between modified Raymer-Hunt transforms with Gulf of Mexico data (after Hartley 1981).

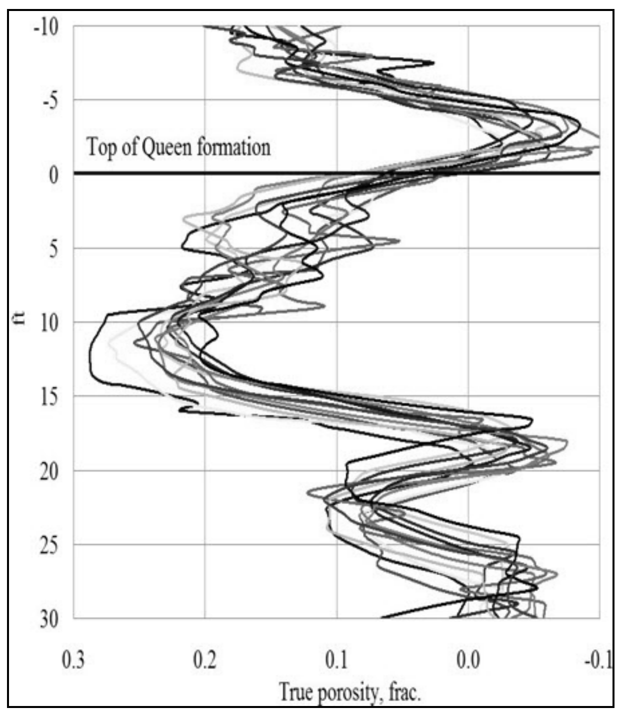

Figure 11 - True porosity from sonic logs

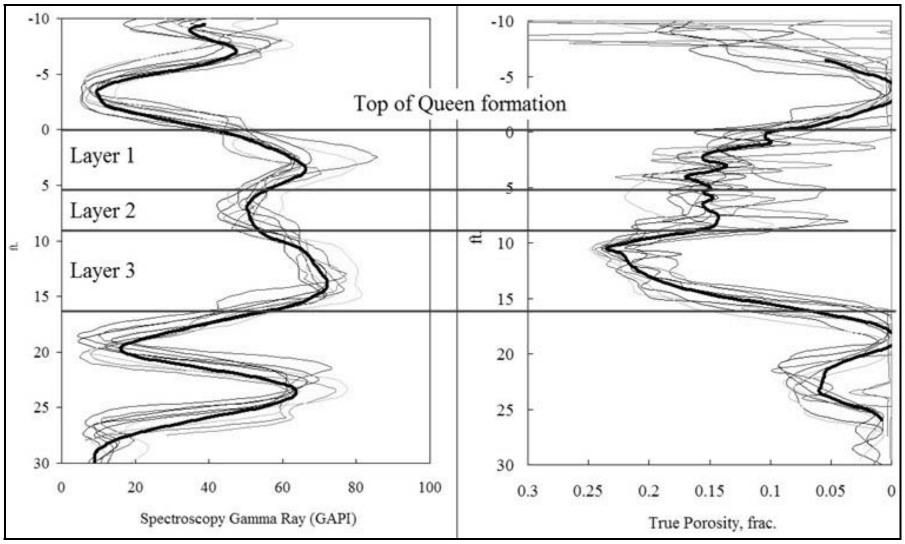

Figure 12 – Layering result from gamma ray and porosity logs of Eskimo State No.1 to 9

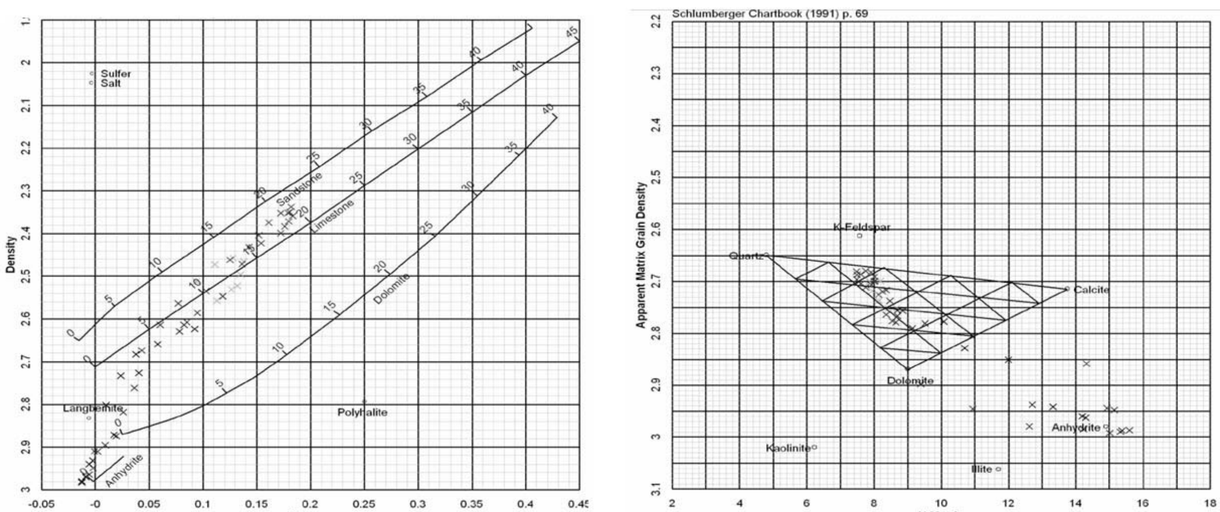

Figure 13 – An example of density/neutron crossplot and lithodensity MID plot from Eskimo State No.2

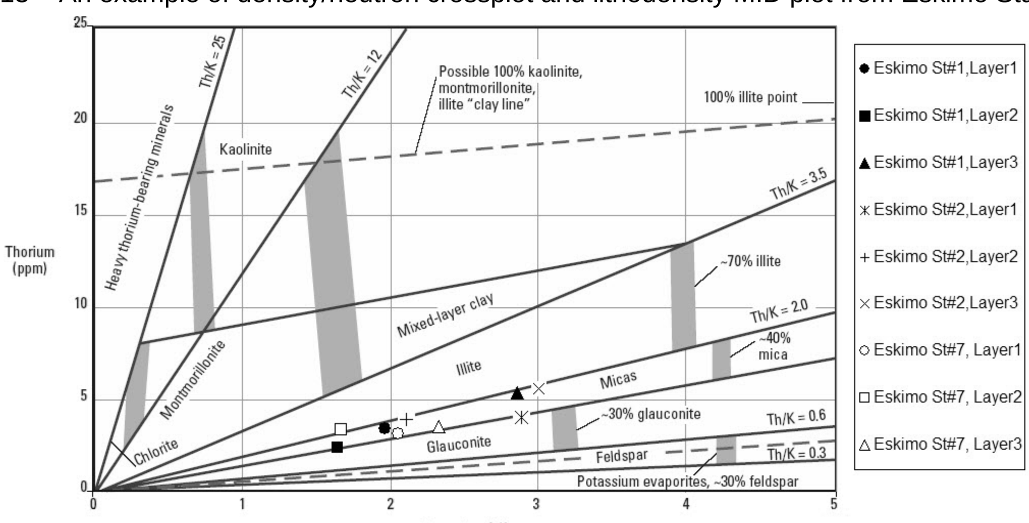

Figure 14 – Schlumberger mineral identification chart plotted along with data from gamma ray spectrometry tool of Eskimo State No.1, No.2, and No.7 (courtesy Schlumberger)

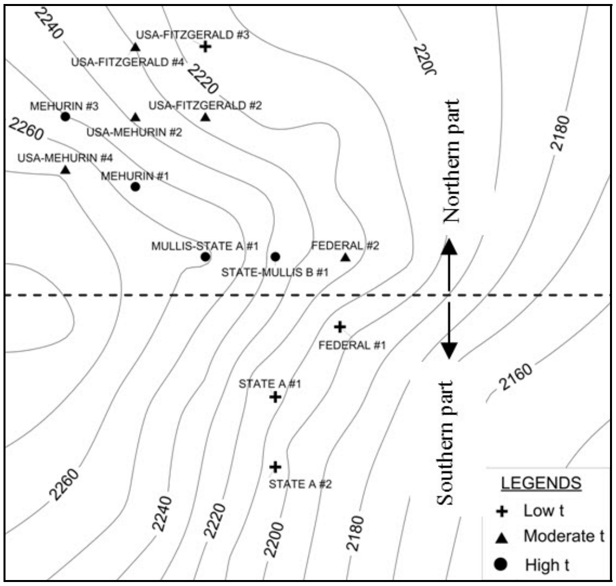

Figure 15 – Friable zone observed from wells with sonic logs

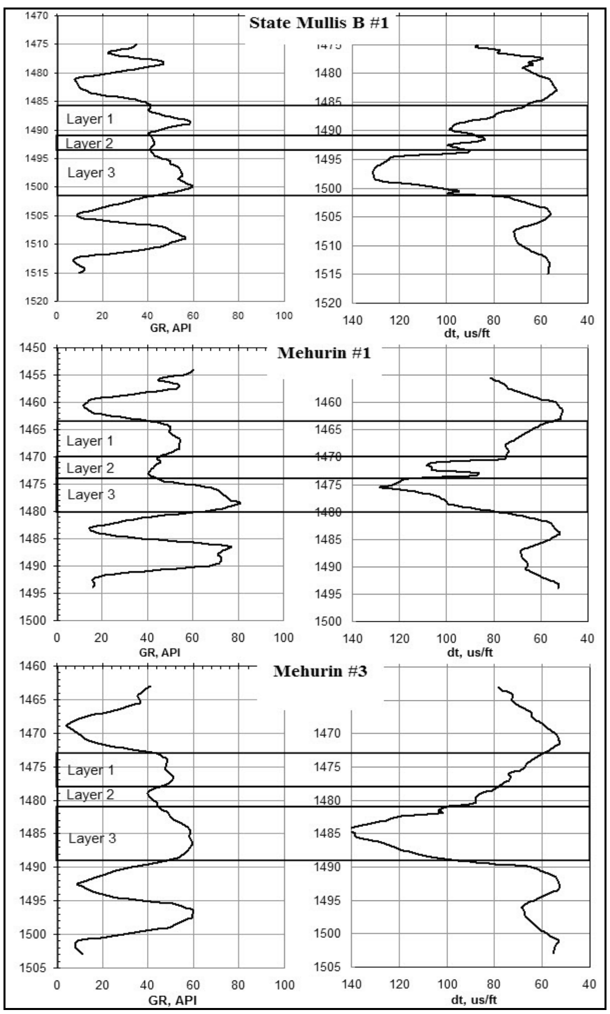

Figure 16 – Rock compaction analysis between layers

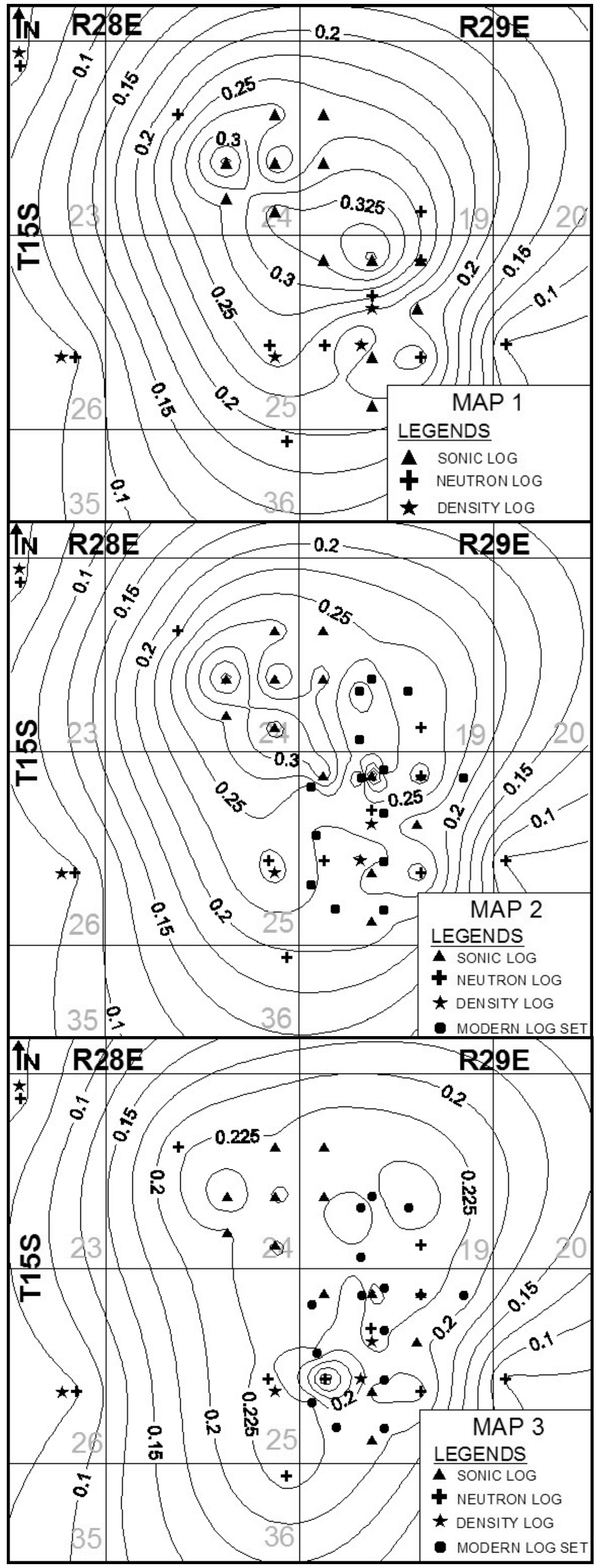

Figure 17 – Porosity maps: Map1; from old logs, Map2; from old logs and modern logs, Map3; from calibrated old logs and modern logs.